

Constraints on a scalar-tensor theory with an intermediate-range force by binary pulsars

DENG Xue-Mei^{1*}

¹*Purple Mountain Observatory, Chinese Academy of Sciences, Nanjing 210008, China*

Searching for an intermediate-range force has been considerable interests in gravity experiments. In this paper, aiming at a scalar-tensor theory with an intermediate-range force, we have derived the metric and equations of motion (EOMs) in the first post-Newtonian (1PN) approximation for general matter without specific equation of state and N point masses firstly. Subsequently, the secular periastron precession $\dot{\omega}$ of binary pulsars in harmonic coordinates is given. After that, $\dot{\omega}$ of four binary pulsars data (PSR B1913+16, PSR B1534+12, PSR J0737-3039 and PSR B2127+11C) have been used to constrain the intermediate-range force, namely, the parameters α and λ . α and λ respectively represent the strength of the intermediate-range force coupling and its length scale. The limits from four binary pulsars data are respectively $\lambda = (4.95 \pm 0.02) \times 10^8 \text{ m}$ and $\alpha = (2.30 \pm 0.01) \times 10^{-8}$ if $\beta = 1$ where β is a parameter like standard parametrized post-Newtonian parameter β_{PPN} . When three degrees of freedom (α , λ and $\bar{\beta} \equiv \beta - 1$) in 1σ confidence level are considered, it yields $\alpha = (4.21 \pm 0.01) \times 10^{-4}$, $\lambda = (4.51 \pm 0.01) \times 10^7 \text{ m}$ and $\bar{\beta} = (-3.30 \pm 0.01) \times 10^{-3}$. Through our research on the scalar-tensor theory with the intermediate-range force, it shows that the parameter α is directly related to the parameter γ ($\alpha = (1 - \gamma)/(1 + \gamma)$). Thus, this presents the constraints on $1 - \gamma$ by binary pulsars which is about 10^{-4} for three degrees of freedom.

PACS: 04.50.-h, 04.25.Nx, 04.80.Cc

1 Introduction

With tremendous advance in the accuracy of observations, Einstein's general relativity (GR) has passed nearly all the tests in the solar system. However, alternative gravity theories are still required for deeper understanding of the nature of spacetime and for testing possible violations of the Einstein equivalence principle (EEP) in the forthcoming more precision level. Among them, a scalar-tensor theory is the most challenging one (see [1] for review). The theory not only has the simplest and most natural way to modify general relativity, but also the presence of a scalar field could explain some exotic phenomena such as the dark energy.

In this paper, we adopt the following modified action for the scalar-tensor theory with an intermediate-range force [2]

$$S = \frac{c^3}{16\pi} \int \left(\phi R - \frac{\theta(\phi)}{\phi} \phi^{\sigma\sigma} \phi_{,\sigma} + 2\phi\lambda(\phi) - \frac{16\pi}{c^4} \mathcal{L}_I(g_{\mu\nu}, \Psi) \right) \sqrt{-g} d^4x, \quad (1)$$

where Ψ denotes all the matter fields. In Eq. (1), the matter fields Ψ only interact with the metric field. This means that

the trajectory of a free-fall test particle depends only on the space-time geometry so that it satisfies the EEP. Although the current experiments verify EEP to a very high accuracy in the Solar System, violations of EEP at galactic and cosmological distance scales can not be ruled out. And discussion about the violations of EEP is beyond the scope of the present paper. $\theta(\phi)$ is the coupling function and the function $\Theta(\phi)$ has the following relationship

$$\Theta(\phi) = \vartheta_2(\phi - \phi_0)^2, \quad (2)$$

which can generate an intermediate-range force. Some experiments give some limits for the intermediate-range force through searching for apparent deviations from Newtonian gravity (see Sec. III. B in Ref. [3]). Especially, a space mission called Phobos Laser Ranging [4] in the near future will detect this effect.

On the other hand, binary pulsars promise an unprecedented opportunity to measure the effects of relativistic grav-

*Corresponding author (email: xmd@pmo.ac.cn)

itation (see [5, 6] for a review). For example, pulsar timing has provided indirect evidence for the existence of gravitational waves [7], the binary pulsars data can constrain the existence of massive black hole binaries [8], and the binary pulsars can also test the effects of strong relativistic internal gravitational fields on orbital dynamics [9]. In addition, binary pulsars could help us to test various gravity theories. By fitting the arrival time of pulsars, observational parameters of binary pulsar are obtained in high precision. It is worthy of note that the periastron advance for binary pulsars could reach several degrees per year, which is about 10^5 more than the perihelion advance of Mercury. Hence, the relativistic effects from binary pulsar are more remarkable than other celestial systems. We will take a sample of binary pulsars for testing the intermediate-range force by using their $\dot{\omega}$. In this paper four best studied pulsar binaries are chosen. They are respectively PSR B1913+16, PSR B1534+12, PSR J0737-3039, and PSR B2127+11C, which are double neutron star binaries. We mainly focus on $\dot{\omega}$ of these four binaries data to constrain the parameters of the intermediate-range force.

In what follows, our conventions and notations generally follow those of [10], and the metric signature is $(-, +, +, +)$. Greek indices take the values from 0 to 3, while Latin indices take the values from 1 to 3. A comma denotes a partial derivative, and semicolon denotes a covariant derivative. Bold letters denote spatial vectors. The plot of this paper is as follows. In Sec. 2, the metric and equations of motion (EOMs) in the first order post-Newtonian (1PN) approximation for general matter without specific equation of state are given by Chandrasekhar's approach. Subsequently, in Sec. 3, we derive the EOMs and $\dot{\omega}$ for binary and discuss two parameters (α and λ) about the intermediate-range force. We then constrain the parameters by means of fitting $\dot{\omega}$ for four binary pulsars and deal with the details of discussion about results in Sec. 4. Finally, constraints method and results are outlined in Sec. 5.

2 The first post-Newtonian approximation

2.1 Field equations by variation

Variation of the action equation Eq. (1) with respect to $g_{\mu\nu}$ yields

$$R_{\mu\nu} = \frac{8\pi}{\phi c^2} \left(T_{\mu\nu} - \frac{1}{2} g_{\mu\nu} T \right) + \frac{\theta(\phi)}{\phi^2} \phi_{,\mu} \phi_{,\nu} + \frac{1}{\phi} \left(\phi_{;\mu\nu} + \frac{1}{2} g_{\mu\nu} \square_g \phi \right) - g_{\mu\nu} \Theta, \quad (3)$$

where $\square_g(\cdot) = (\cdot)_{;\alpha\beta} g^{\alpha\beta}$. $T_{\mu\nu}$ is the stress-energy-momentum tensor of matter defined as

$$\frac{c^2}{2} \sqrt{-g} T_{\mu\nu} \equiv \frac{\partial(\sqrt{-g} \mathcal{L}_I)}{\partial g^{\mu\nu}} - \frac{\partial}{\partial x^\alpha} \frac{\partial(\sqrt{-g} \mathcal{L}_I)}{\partial g_{,\alpha}^{\mu\nu}}. \quad (4)$$

Following [11, 12, 13], mass, current, and stress density can be defined as

$$\sigma \equiv T^{00} + T^{kk}, \quad (5)$$

$$\sigma_i \equiv c T^{0i}, \quad (6)$$

$$\sigma_{ij} \equiv c^2 T^{ij}. \quad (7)$$

It is worth emphasizing that, in these definitions, the matter is described by the energy-momentum tensor without specific equation of state. Variation of the action with respect to ϕ yields

$$\square_g \phi = \frac{1}{3 + 2\theta(\phi)} \left(\frac{8\pi}{c^2} T - \phi_{,\alpha} \phi^{,\alpha} \frac{d\theta}{d\phi} - 2\phi^2 \frac{d\Theta}{d\phi} + 2\phi\Theta \right). \quad (8)$$

2.2 Perturbation of the scalar-tensor theory with the intermediate-range force

Following the approach in [14], we deal with the metric tensor in the form of a Taylor expansion in the parameter $\epsilon \equiv 1/c$ as follows

$$g_{00} = -1 + \epsilon^2 N + \epsilon^4 L + \mathcal{O}(5), \quad (9)$$

$$g_{0i} = \epsilon^3 L_i + \mathcal{O}(5), \quad (10)$$

$$g_{ij} = \delta_{ij} + \epsilon^2 H_{ij} + \mathcal{O}(4), \quad (11)$$

$\mathcal{O}(n)$ means the order of ϵ^n . We assume that the scalar field can be expanded in power series around its background value ϕ_0 as Kopeikin and Vlasov [15] and define

$$\phi = \phi_0(1 + \zeta), \quad (12)$$

where ζ is dimensionless perturbation of the scalar field around ϕ_0 .

In particular, decomposition of the coupling function $\theta(\phi)$ can be written as

$$\theta(\phi) = \omega_0 + \omega_1 \zeta + \dots, \quad (13)$$

$$\zeta = \epsilon^2 \zeta^{(2)} + \dots \quad (14)$$

where $\omega_0 \equiv \theta(\phi_0)$ and $\omega_n \equiv (d^n \theta / d\zeta^n)_{\phi=\phi_0}$. According to Eqs. (12), (13) and (14), we have

$$\theta(\phi) = \omega_0 + \epsilon^2 \omega_1 \zeta^{(2)} + \mathcal{O}(4), \quad (15)$$

$$\frac{d\theta}{d\phi} = \frac{1}{\phi_0} \left(\omega_1 + \mathcal{O}(2) \right). \quad (16)$$

Now two parameters γ and β are introduced as follows:

$$\gamma \equiv \frac{\omega_0 + 1}{\omega_0 + 2}, \quad (17)$$

$$\beta \equiv 1 + \frac{\omega_1}{(2\omega_0 + 3)(2\omega_0 + 4)^2}. \quad (18)$$

$$(19)$$

For scalar-tensor theory with $\theta_2 = 0$, it turns out that γ and β become the values of corresponding standard PPN parameters γ_{PPN} and β_{PPN} [16, 17].

2.3 Gauge condition and the first post-Newtonian approximation

We use the gauge condition imposed on the component of the metric tensor proposed by Kopeikin & Vlasov [15] as follows:

$$\left(\frac{\phi}{\phi_0} \sqrt{-g} g^{\mu\nu}\right)_{, \nu} = 0. \quad (20)$$

To 1PN order, this gauge gives

$$\epsilon^2 \left(\frac{1}{2} H_{,i} - \frac{1}{2} N_{,i} - H_{ik,k} + \zeta_{,i}^{(2)} \right) = 0, \quad (21)$$

and

$$\epsilon^3 \left(-\frac{1}{2} N_{,t} - \frac{1}{2} H_{,t} + L_{k,k} - \zeta_{,t}^{(2)} \right) = 0. \quad (22)$$

Based on fields equations, their perturbation and the gauge conditions, the results are obtained as follows.

The equations for N and $\zeta^{(2)}$ are

$$\square N + \xi_1 \zeta^{(2)} = -8\pi G\sigma, \quad (23)$$

and

$$\square \zeta^{(2)} + \xi_1 \zeta^{(2)} = -4(1-\gamma)\pi G\sigma, \quad (24)$$

where \square is the D'Alembert operator in the Minkowski spacetime. And

$$\xi_1 = 4 \frac{1-\gamma}{1+\gamma} \vartheta_2 \phi_0^2. \quad (25)$$

For 1PN approximation, it yields

$$\square H_{ij} = \delta_{ij}(-8\gamma\pi G\sigma + \xi_1 \zeta^{(2)}), \quad (26)$$

which gives $H_{ij} = V\delta_{ij}$ and $G \equiv 2/[\phi_0(1+\gamma)]$ so that

$$\square V - \xi_1 \zeta^{(2)} = -8\gamma\pi G\sigma, \quad (27)$$

and

$$\square L_i = 8(\gamma+1)\pi G\sigma_i, \quad (28)$$

$$\begin{aligned} \square L + \xi_1 \zeta^{(4)} &= -8\pi G\sigma \left(V - 2N + \frac{4\beta - \gamma - 3}{\gamma - 1} \zeta^{(2)} \right) \\ &\quad - 8(\gamma - 1)\pi G\sigma_{kk} - \frac{1}{2} N_{,k} N_{,k} - \frac{1}{2} N_{,k} V_{,k} \\ &\quad - \zeta_{,k}^{(2)} N_{,k} - \frac{4(\beta - 1)}{(\gamma - 1)^2} \zeta_{,k}^{(2)} \zeta_{,k}^{(2)} \\ &\quad + \xi_1 (N - V) \zeta^{(2)} - \xi_3 \zeta^{(2)^2}, \end{aligned} \quad (29)$$

$$\begin{aligned} \square \zeta^{(4)} + \xi_1 \zeta^{(4)} &= -4\pi G\sigma \left[(\gamma - 1)(N - V) + \frac{8(\beta - 1)}{\gamma - 1} \zeta^{(2)} \right] \\ &\quad - 8(\gamma - 1)\pi G\sigma_{kk} + \frac{1}{2} \zeta_{,k}^{(2)} N_{,k} - \frac{1}{2} \zeta_{,k}^{(2)} V_{,k} \\ &\quad + \frac{4(1 - \beta)}{(\gamma - 1)^2} \zeta_{,k}^{(2)} \zeta_{,k}^{(2)} - \xi_1 V \zeta^{(2)} + \xi_2 \zeta^{(2)^2}, \end{aligned} \quad (30)$$

where

$$\xi_2 = 2 \frac{3\gamma^2 - 6\gamma - 16\beta + 19}{\gamma^2 - 1} \vartheta_2 \phi_0^2, \quad (31)$$

and

$$\xi_3 = 4 \frac{8\beta + \gamma - 9}{\gamma^2 - 1} \vartheta_2 \phi_0^2. \quad (32)$$

2.4 Equations of motion in 1PN

$T_{;\nu}^{i\nu} \equiv 0$ yields the momentum equation

$$\begin{aligned} &\sigma_{i,t} + \sigma_{ik,k} - \frac{1}{2} \sigma N_{,i} \\ &+ \epsilon^2 \left(\frac{1}{2} \sigma V N_{,i} + \sigma L_{i,t} - \frac{1}{2} \sigma L_{,i} \right. \\ &+ \frac{5}{2} \sigma_i V_{,t} - \frac{1}{2} \sigma_i N_{,t} + \sigma_k L_{i,k} - \sigma_k L_{k,i} \\ &\left. + \frac{5}{2} \sigma_{ik} V_{,k} - \frac{1}{2} \sigma_{ik} N_{,k} + \frac{1}{2} \sigma_{kk} N_{,i} - \frac{1}{2} \sigma_{kk} V_{,i} \right) = 0. \end{aligned} \quad (33)$$

$T_{;\nu}^{0\nu} \equiv 0$ yields the continuity equation

$$\begin{aligned} &\sigma_{,t} + \sigma_{k,k} \\ &+ \epsilon^2 \left(\frac{3}{2} V_{,t} \sigma - N_{,t} \sigma + \frac{3}{2} V_{,k} \sigma_k - N_{,k} \sigma_k - \sigma_{kk,t} \right) = 0. \end{aligned} \quad (34)$$

3 N-body pointlike and secular periastron precession of binary pulsar in 1PN

Considering an N-body system of nonspinning point masses for simplicity, we follow the notation adopted by [18] and use the matter stress energy tensor as follows

$$c^2 T^{\mu\nu}(\mathbf{x}, t) = \sum_a \mu_a(t) v_a^\mu v_a^\nu \delta(\mathbf{x} - \mathbf{y}_a(t)), \quad (35)$$

where δ denotes the three-dimensional Dirac distribution, the trajectory of the a th mass is represented by $\mathbf{y}_a(t)$, the coordinate velocities of the a th body are $\mathbf{v}_a = d\mathbf{y}_a(t)/dt$ and $v_a^\mu \equiv (c, \mathbf{v}_a)$, and μ_a denotes an effective time-dependent mass of the a th body defined by

$$\mu_a(t) = \left(\frac{m_a}{\sqrt{g g_{\rho\sigma} \frac{v_a^\rho v_a^\sigma}{c^2}}} \right)_a, \quad (36)$$

where subscript a denotes evaluation at the a th body and m_a is the constant Schwarzschild mass. Another useful notation is

$$\tilde{\mu}_a(t) = \mu_a(t) \left[1 + \frac{v_a^2}{c^2} \right], \quad (37)$$

where $v_a^2 = \mathbf{v}_a^2$. Both μ_a and $\tilde{\mu}_a$ reduce to the Schwarzschild mass at Newtonian order: $\mu_a = m_a + \mathcal{O}(\epsilon^2)$ and $\tilde{\mu}_a = m_a + \mathcal{O}(\epsilon^2)$. Then the mass, current, and stress densities in Eqs. (5), (6) and (7) for the N point masses read

$$\sigma = \sum_a \tilde{\mu}_a \delta(\mathbf{x} - \mathbf{y}_a(t)), \quad (38)$$

$$\sigma_i = \sum_a \mu_a v_a^i \delta(\mathbf{x} - \mathbf{y}_a(t)), \quad (39)$$

$$\sigma_{ij} = \sum_a \mu_a v_a^i v_a^j \delta(\mathbf{x} - \mathbf{y}_a(t)). \quad (40)$$

It can be written as the following form in Newtonian approximation,

$$N - \overset{(2)}{\zeta} = (1 + \gamma)\Delta^{-1}\{-4\pi G\sigma\} = (1 + \gamma) \sum_a \frac{Gm_a}{r_a} + O(2), \quad (41)$$

and

$$\begin{aligned} \overset{(2)}{\zeta} &= (1 - \gamma)G \int \frac{e^{-\sqrt{-\xi_1}|\mathbf{x}-\mathbf{z}|}}{|\mathbf{x}-\mathbf{z}|} \sigma d^3\mathbf{z} \\ &= (1 - \gamma) \sum_a \frac{Gm_a}{r_a} e^{-\frac{r_a}{\lambda}}, \end{aligned} \quad (42)$$

$$\text{where } \lambda = \frac{1}{\sqrt{-\xi_1}} = \left[2\phi_0 \sqrt{\frac{\gamma-1}{\gamma+1}} \vartheta_2\right]^{-1}.$$

Then, we derive

$$N = (1 + \gamma) \sum_a \frac{Gm_a}{r_a} + (1 - \gamma) \sum_a \frac{Gm_a}{r_a} e^{-\frac{r_a}{\lambda}}. \quad (43)$$

Through integration of Eq. (33), EOMs in Newtonian approximation are given as follows

$$\frac{dv_a^i}{dt} = - \sum_{b \neq a} \frac{Gm_b}{r_{ab}^3} r_{ab}^i \left\{ \frac{1 + \gamma}{2} + \frac{1 - \gamma}{2} e^{-r_{ab}/\lambda} \left(1 + \frac{r_{ab}}{\lambda} \right) \right\}. \quad (44)$$

From Eq. (44), the gravitational potential in Newtonian approximation is

$$U(r) = - \sum_{b \neq a} \frac{Gm_b}{r_{ab}} \left(\frac{1 + \gamma}{2} + \frac{1 - \gamma}{2} e^{-\frac{r_{ab}}{\lambda}} \right). \quad (45)$$

On the other hand, Fischbach and Talmadge [19] provided the following potential

$$U(r)_{FT} = - \sum_{b \neq a} \frac{Gm_b}{r_{ab}} \left(1 + \alpha e^{-\frac{r_{ab}}{\lambda}} \right), \quad (46)$$

which includes a usual Newtonian gravitational potential and a Yukawa-type one which could explain the intermediate-range force. Through comparing Eq. (45) and Eq. (46), we define $\mathcal{G} \equiv (1 + \gamma)G/2$ and $\alpha \equiv (1 - \gamma)/(1 + \gamma)$. It shows that the parameter α is directly related to the parameter γ . If we constrain on α by binary pulsars, it will limit on the value of the parameter γ in turn. Besides, a plus or minus sign before α denotes an attractive or repulsive force provided by the intermediate-range force. Then, Eq. (44) becomes

$$\frac{dv_a^i}{dt} = - \sum_{b \neq a} \frac{Gm_b}{r_{ab}^3} r_{ab}^i \left\{ 1 + \alpha e^{-r_{ab}/\lambda} \left(1 + \frac{r_{ab}}{\lambda} \right) \right\} + O(2). \quad (47)$$

The next step is to work out N and V easily in 1PN approximation as

$$N = 2 \sum_a \frac{Gm_a}{r_a} + 2\alpha \sum_a \frac{Gm_a}{r_a} e^{-r_a/\lambda}$$

$$\begin{aligned} &+ \epsilon^2 \left\{ \sum_a \frac{Gm_a}{r_a} \left[4v_a^2 - (n_a v_a)^2 \right] \right. \\ &- 2 \sum_a \sum_{b \neq a} \frac{\mathcal{G}^2 m_a m_b}{r_a r_{ab}} \left[1 - 5\alpha e^{-r_{ab}/\lambda} \right] \\ &\left. + \sum_a \sum_{b \neq a} \frac{\mathcal{G}^2 m_a m_b}{r_{ab}^2} (n_a n_{ab}) \right\} + O(3), \end{aligned} \quad (48)$$

$$V = 2 \sum_a \frac{Gm_a}{r_a} - 2\alpha \sum_a \frac{Gm_a}{r_a} e^{-\frac{r_a}{\lambda}} + O(2), \quad (49)$$

by the relation of $\tilde{\mu}_a$ that

$$\begin{aligned} \tilde{\mu}_a &= m_a \left\{ 1 + \epsilon^2 \left[\left(N - \frac{3}{2}V \right)_a + \frac{3}{2}v_a^2 \right] + O(4) \right\} \\ &= m_a \left\{ 1 + \epsilon^2 \left[- \sum_{b \neq a} \frac{Gm_b}{r_{ab}} + 5\alpha \sum_{b \neq a} \frac{Gm_b}{r_{ab}} e^{-r_{ab}/\lambda} \right. \right. \\ &\left. \left. + \frac{3}{2}v_a^2 \right] + O(4) \right\}, \end{aligned} \quad (50)$$

where $r_a = |\mathbf{x} - \mathbf{y}_a|$ and $r_{ab} = |\mathbf{y}_a - \mathbf{y}_b|$. For L_i ,

$$L_i = -4 \sum_a \frac{Gm_a}{r_a} v_a^i + O(2). \quad (51)$$

Because intermediate-range force in the Newtonian order is very tiny (see reference [3]), we omit any coupling terms in the magnitude of $\alpha^2 \epsilon^2$, $\epsilon^2 e^{-r_a/\lambda}$ and drop out the terms including coefficients of ξ_2 and ξ_3 . Thus, it yields

$$\begin{aligned} L &= 4(1 - \beta - \alpha - 2\alpha\beta) \sum_a \sum_{b \neq a} \frac{\mathcal{G}^2 m_a m_b}{r_a r_{ab}} - 4\alpha \sum_a \frac{Gm_a}{r_a} v_a^2 \\ &- 2\beta(1 + 2\alpha) \sum_a \sum_b \frac{\mathcal{G}^2 m_a m_b}{r_a r_b} + O(1, \alpha^2, e^{-r_a/\lambda}). \end{aligned} \quad (52)$$

At last, by integration of Eq. (33), EOMs in 1PN are obtained:

$$\begin{aligned} \frac{dv_a^i}{dt} &= - \sum_{b \neq a} \frac{Gm_b}{r_{ab}^2} n_{ab}^i - \alpha \sum_{b \neq a} \frac{Gm_b}{r_{ab}^2} n_{ab}^i \left(1 + \frac{r_{ab}}{\lambda} \right) e^{-r_{ab}/\lambda} \\ &+ \epsilon^2 \left\{ 2(1 + \beta + 2\alpha\beta) \sum_{b \neq a} \frac{\mathcal{G}^2 m_b^2}{r_{ab}^3} n_{ab}^i \right. \\ &+ (3 + 2\beta - 3\alpha + 4\alpha\beta) \sum_{b \neq a} \frac{\mathcal{G}^2 m_a m_b}{r_{ab}^3} n_{ab}^i \\ &+ \sum_{b \neq a} \frac{Gm_b}{r_{ab}^2} \left[- \left(1 - \frac{1}{2} \alpha \right) v_a^2 - 2(1 - \alpha) v_b^2 + \frac{3}{2} (n_{ab} v_b)^2 \right. \\ &\left. + 4(v_a v_b) \right] n_{ab}^i + \sum_{b \neq a} \frac{Gm_b}{r_{ab}^2} \left[4(n_{ab} v_a) \right. \\ &\left. - 3(n_{ab} v_b) \right] v_{ab}^i - \alpha \sum_{b \neq a} \frac{Gm_b}{r_{ab}^2} (n_{ab} v_{ab}) v_a^i \\ &\left. + \sum_{b \neq a} \sum_{c \neq a, b} \frac{\mathcal{G}^2 m_b m_c}{r_{ab}^2} \left[(2\beta - 1 - 3\alpha + 4\alpha\beta) \frac{1}{r_{bc}} \right. \right. \end{aligned}$$

$$+2(1 + \beta + 2\alpha\beta)\frac{1}{r_{ac}} - \frac{1}{2}\frac{r_{ab}}{r_{bc}^2}(n_{bc}n_{ab})\Big]n_{ab}^i - \frac{7}{2}\sum_{b \neq a} \sum_{c \neq a,b} \frac{\mathcal{G}^2 m_b m_c}{r_{ab} r_{bc}^2} n_{bc}^i \Big\} + \mathcal{O}(\epsilon^4, \epsilon^2 \alpha e^{-r/\lambda}, \epsilon^2 \alpha^2) \quad (53)$$

where $n_{ab}^i = (y_a^i - y_b^i)/r_{ab}$, $\mathbf{v}_{ab} = \mathbf{v}_a - \mathbf{v}_b$, and scalar products are denoted with parentheses, e. g., $(n_{ab}v_{ab}) = \mathbf{n}_{ab} \cdot \mathbf{v}_{ab}$. Eq. (53) will return to Einstein-Infeld-Hoffmann (EIH) equations of motion [20] with $\beta = 1$ when we eliminate the contribution of the intermediate-range force ($\alpha = 0$).

When only two bodies (m_1 and m_2) in Eq. (53) are considered, EOMs of a point-mass binary in 1PN yield

$$\ddot{\mathbf{r}} = \mathbf{a}_N + \mathbf{a}_{1PN}, \quad (54)$$

$$\begin{aligned} \mathbf{a}_N &= -\frac{\mathcal{G}M}{r^2} \left[1 + \alpha \left(1 + \frac{r}{\lambda} \right) \exp\left(-\frac{r}{\lambda}\right) \right] \mathbf{n}, \quad (55) \\ \mathbf{a}_{1PN} &= -\frac{\mathcal{G}M}{c^2 r^2} \left\{ \left[\left(1 + 3v - \frac{1}{2}\alpha v - \frac{1}{2}\alpha \right) v^2 - 2 \left(1 + \beta + v + 2\alpha\beta + 3\alpha v \right) \frac{\mathcal{G}M}{r} - \frac{3}{2}v\dot{r}^2 \right] \mathbf{n} - \left(4 - 2v - \alpha + 2\alpha v \right) \dot{r} \mathbf{v} \right\}, \quad (56) \end{aligned}$$

where $M = m_1 + m_2$, $\dot{r} = (n_{12}v_{12})$, $\mathbf{v} = \mathbf{v}_1 - \mathbf{v}_2$, $v = m_1 m_2 / M^2$, $\mathbf{r} = \mathbf{r}_{12}$, $\mathbf{n} = \mathbf{n}_{12}$ and $\mathbf{a} = d\mathbf{v}_{12}/dt$. Comparing our results with the ones of [21], we can see another additional term comes from the intermediate-range force in Eq. (54). By the aid of the averaging method, the secular periastron advance for a binary pulsar in 1PN is

$$\frac{d\omega}{dt} = \frac{1}{2} \frac{n\alpha p^2}{\lambda^2} e^{-p/\lambda} + \left(4 - \beta - \frac{3}{2}\alpha - 2\alpha\beta - \frac{3}{2}\alpha v \right) \frac{\mathcal{G}Mn}{p} \epsilon^2, \quad (57)$$

where $n^2 a^3 = GM$, $p = a(1 - e^2)$, a is the semi-major axis and e is the eccentricity of the binary. It is worthy of note that there exists the contribution of the intermediate-range force in Eq. (57). When we drop out its effect ($\alpha = 0$), Eq. (57) will return to the usual result for the general relativity.

4 Constraints on the parameters by binary pulsars

Binary pulsars provide us more impressive tests of general relativity than other systems. For example the fraction will merge due to gravitational wave emission. Besides, a neutron star is rather compact and its companion hardly affects its shape. These systems are highly valuable for measuring the effects of gravity and testing gravitational theories. Four samples used in this paper are PSR B1913+16, PSR B1534+12, PSR J0737-3039 and PSR B2127+11C which are listed in Table 1. The numbers inside a pair of parentheses are the 1σ error of its corresponding quantity. PSR B1913+16 is discovered in 1974 by using the Arecibo 305m antenna [26]. The orbit has evolved since the binary system was initially discovered, in precise agreement with the loss of energy due to

gravitational wave emission predicted by Einstein's General Theory of Relativity. PSR B2127+11C is located in the globular cluster Messier 15. This system appears to be a clone of PSR B1913+16 (see Table 1). For PSR B1534+12, its pulses are significantly stronger and narrower than those of PSR B1913+16 [23]. PSR J0737-3039 was discovered during a pulsar search carried out using a multibeam receiver with 64m radio telescope in 2003 [24]. And this system has shorter orbital period, smaller eccentricity and larger periastron advance. When $\beta = 1$, each $\dot{\omega}$ in Table 1 will confine the values of α and λ in a curve through Eq.(57) (see Fig. 1 and Fig. 2).

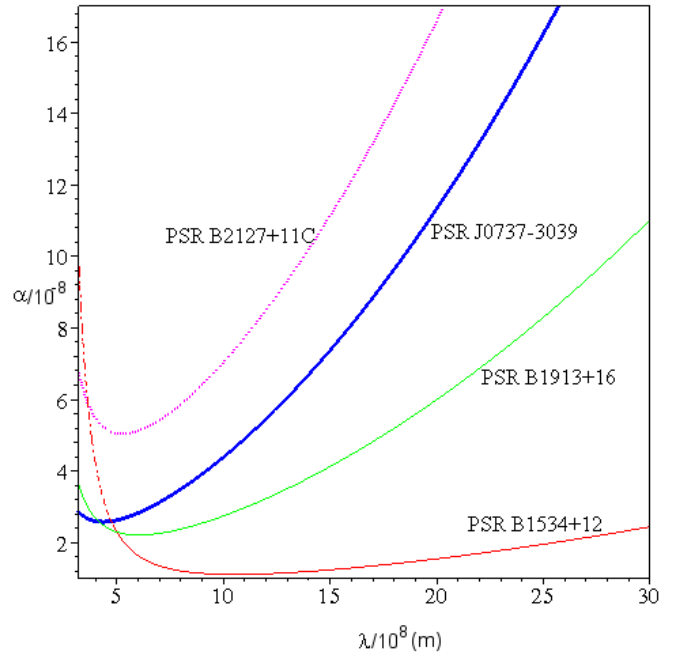


Figure 1 The plane of λ - α constrained by $\dot{\omega}$ of four double neutron star binaries, where the real line (green) denotes PSR B1913+16, the thinnest dashed line (red) denotes PSR B1534+12, the thickest dashed line (blue) denotes PSR J0737-3039, and the dotted line (magenta) denotes PSR B2127+11C. It can be seen that the four curves are nearly cross at one point.

In Fig. 1, the trajectories of four double neutron star binaries in the plane of the parameters α and λ have been shown. From Fig. 1, the three trajectories almost meet together. Fig. 2 is the enlarged drawing of Fig. 1 at a smaller scale.

Table 1: Parameters in binary pulsars.

Pulsars	e	$m_1 (M_\odot)$	$m_2 (M_\odot)$	P (day)	$\langle \dot{\omega} \rangle$ ($^\circ\text{yr}^{-1}$)	Ref.
PSR B1913+16	0.6171338(4)	1.3873(3)	1.4408(3)	0.322997462727(5)	4.226595(5)	[22]
PSR B1534+12	0.2736767(1)	1.3452(1)	1.3332(1)	0.420737299153(4)	1.755805(3)	[23]
PSR J0737-3039	0.0877775(9)	1.250(5)	1.337(5)	0.10225156248(5)	16.89947(68)	[24]
PSR B2127+11C	0.681395(2)	1.358(10)	1.354(10)	0.33528204828(5)	4.4644(1)	[25]

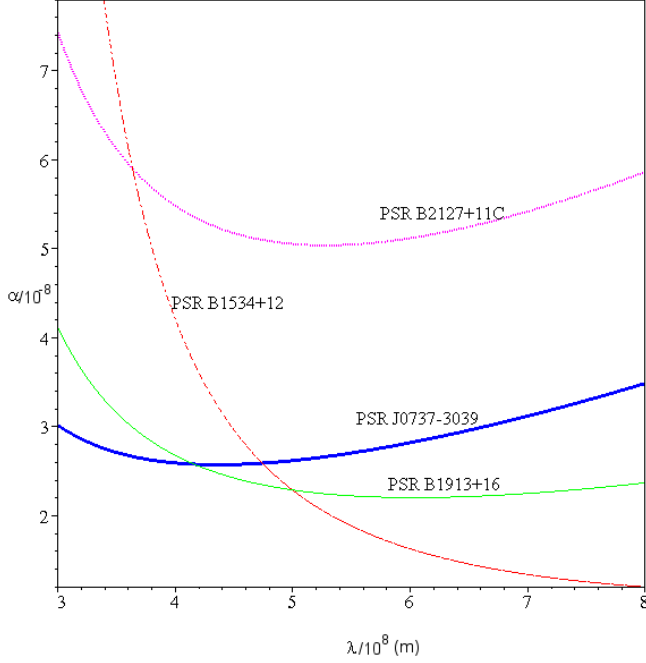


Figure 2 The enlarged diagram of the region around the cross point in Figure 1. The legend is the same as in Figure 1.

On the other hand, Damour & Esposito-Farèse [12] constrain two 2PN parameters of Multi-Scalar-Tensor theory by using four different binary pulsars data in 1σ confidence level. Using the same method of [12], we constrain the parameters of the intermediate-range force in 1σ confidence level. Firstly, an 1σ constraint imposed by double neutron star binaries is plotted. Each set of binary data leads to a reduced χ^2 : $\chi_{binary}^2(\alpha, \lambda) = (\dot{\omega}_{theory} - \dot{\omega}_{observation})^2 / \sigma_{observation}^2$, equivalent to the 1σ constraint $-\sigma_{observation} < \dot{\omega}_{theory} - \dot{\omega}_{observation} < \sigma_{observation}$. The bounds by four double neutron star binaries allowed regions of the λ - α plane are displayed in Fig. 3. Clearly four binaries data favor only a small region of the parameters. To combine the constraints on α and λ coming from different double neutron star binaries experiments, their individual χ^2 have been added as if they were part of a total experiment with uncorrelated Gaussian errors like the analysis method of [12]: $\chi_{total}^2(\alpha, \lambda) = \chi_{1913+16}^2(\alpha, \lambda) + \chi_{1534+12}^2(\alpha, \lambda) + \chi_{0737-3039}^2(\alpha, \lambda) + \chi_{2127+11C}^2(\alpha, \lambda)$. Therefore, it can be plotted at the contour level $\Delta\chi_{total}^2(\alpha, \lambda) =$

2.3, $\Delta\chi_{total}^2(\alpha, \lambda) = 6.17$, and $\Delta\chi_{total}^2(\alpha, \lambda) = 11.8$, where $\Delta\chi_{total}^2(\alpha, \lambda) = \chi_{total}^2(\alpha, \lambda) - (\chi_{total}^2(\alpha, \lambda))_{min}$, defines respectively for two degrees of freedom the 68.3%, 95.4% and 99.73% confidence levels represented in Fig. 4. The 1σ fit values for the parameters are $\lambda = (4.95 \pm 0.02) \times 10^8\text{m}$ and $\alpha = (2.30 \pm 0.01) \times 10^{-8}$ with $\chi^2 = 28.54$ in the case of $\beta = 1$. When three degrees of freedom (α , λ and $\bar{\beta} \equiv \beta - 1$) are considered in 1σ level, it yields the bounds: $\alpha = (4.21 \pm 0.01) \times 10^{-4}$, $\lambda = (4.51 \pm 0.01) \times 10^7\text{m}$ and $\bar{\beta} = (-3.30 \pm 0.01) \times 10^{-3}$.

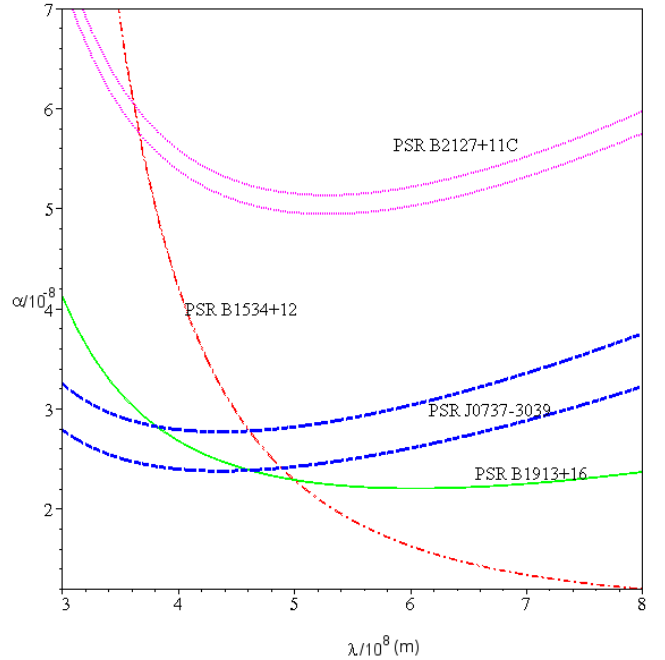


Figure 3 Each curve in Fig.2 is separated into two curves to show the bounds due to the observational 1σ error. Please read the context for the details. Figure legend is the same as in Figure 1.

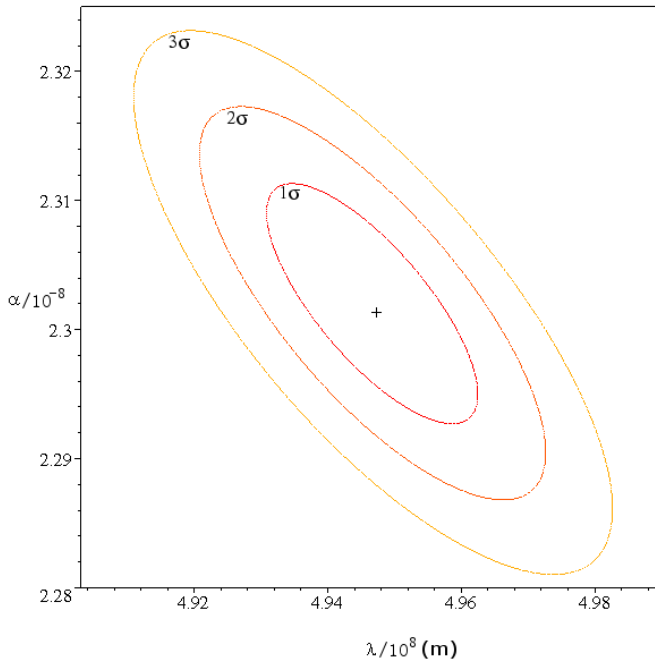


Figure 4 Confidence level contours of 68.3%, 95.4% and 99.73% in the plane of λ - α constrained by four double neutron star binaries. The plus sign denotes the 68.3% values for the parameters of the intermediate-range force which are: $\lambda = (4.95 \pm 0.02) \times 10^8 \text{m}$ and $\alpha = (2.30 \pm 0.01) \times 10^{-8}$, the minimum value of χ^2 is 28.54.

5 Conclusions and prospects

Starting with the action of a scalar-tensor theory with an intermediate-range force, we obtain its equations of motion in the first post-Newtonian order (1PN) for general matter without specific equation of state and N point masses. The secular periastron shift for binary pulsar in 1PN is derived. From the results of the theory in 1PN, there are three parameters: β and two intermediate-range parameters α and λ . Furthermore, with the precondition of $\beta = 1$, α and λ with applied 4 double neutron star binaries data (PSR B1913+16, PSR B1534+12, PSR J0737-3039, PSR B2127+11C) are constrained: $\lambda = (4.95 \pm 0.02) \times 10^8 \text{m}$ and $\alpha = (2.30 \pm 0.01) \times 10^{-8}$. On the other hand, the parameter λ is related to the coupling strength between the scalar field and intermediate-range force, namely, $\phi_0^2 \vartheta_2$. It yields $|\phi_0^2 \vartheta_2| \approx 4.44 \times 10^{-11} \text{m}^2$. Then, instead of the prior of $\beta = 1$, we constrain $\alpha = (4.21 \pm 0.01) \times 10^{-4}$, $\lambda = (4.51 \pm 0.01) \times 10^7 \text{m}$ and $\bar{\beta} \equiv \beta - 1 = (-3.30 \pm 0.01) \times 10^{-3}$ when three degrees of freedom (α , λ and $\bar{\beta}$) are considered in 1σ confidence level. By the relationship between α and γ , it can also give us that $1 - \gamma \approx 10^{-4}$ by binary pulsars data. In addition, $\dot{\mathcal{G}}/\mathcal{G}$ could be constrained by lunar laser ranging. Then, the background value of scalar field could also be constrained though $\mathcal{G} = 1/\phi_0$. Our results show that the limits of binary pulsars systems on the intermediate-range force

are basically consistent with the results from the solar system such as the earth-satellite measurement of earth gravity, the lunar orbiter measurement of lunar gravity, and lunar laser ranging measurement to constrain the force [19, 27]. To solidify the existence of these effects by binary pulsars systems in the future, the timing model should be constructed in the framework of the scalar-tensor theory with the intermediate-range force.

X.-M.Deng is grateful to Prof. Sergei Kopeikin for his useful discussion. X.-M. Deng appreciates the support from the group of Almanac and Astronomical Reference Systems in the Purple Mountain Observatory of China.

- 1 Fujii Y., Maeda K. *The Scalar-Tensor Theory of Gravitation*. Cambridge: Cambridge University Press, 2005
- 2 Xie Y., Ni W-T, Dong P., Huang T-Y, Second post-Newtonian approximation of scalar-tensor theory of gravity. *Advances in Space Research*, 2009, 43:171–180
- 3 Deng X-M, Xie Y., Huang T-Y, A Modified Scalar-Tensor-Vector Gravity Theory and the Constraint on its Parameters. *Phys Rev D*, 2009, 79, 044014
- 4 Turyshev S. G., et al, Advancing tests of relativistic gravity via laser ranging to phobos. *Experimental Astronomy*, 2010, 28:209–249
- 5 Stairs I. H., Pulsars in binary systems: probing binary stellar evolution and general relativity. *Science*, 2004, 304: 547–552
- 6 Lorimer D. R., Binary and millisecond pulsars. *Living Rev Relativity*, 2005, 8, 7
- 7 Detweiler S. L., Pulsar timing measurements and the search for gravitational waves. *Astrophys J*, 1979, 234:1100–1104
- 8 Lommen A. N., Backer D. C., Using pulsars to detect massive black hole binaries via gravitational radiation: sagittarius A* and nearby galaxies. *Astrophys J*, 2001, 562:297–302
- 9 Bell J. F., Camilo F., Damour T., A tighter test of the local Lorentz invariance of gravity using PSR J2317+1439. *Astrophys J*, 1996 464:857
- 10 Misner C.W., Thorne K. S., Wheeler J. A. *Gravitation*. Freeman: San Francisco Press, 1973
- 11 Blanchet L., Damour T., Post-Newtonian generation of gravitational waves. *Ann. Inst. Henri Poincaré*, 1989, 50:377–408
- 12 Damour T., Esposito-Farèse G., Tensor-scalar gravity and binary-pulsar experiments. *Phys Rev D*, 1996, 53, 5541
- 13 Damour T., Esposito-Farèse G., Tensor-multi-scalar theories of gravitation. *Classical Quantum Gravity* 1992, 9:2093–2176
- 14 Chandrasekhar S., The post-Newtonian equations of hydrodynamics in general relativity. *Astrophys J*, 1965, 142:1488
- 15 Kopeikin S., Vlasov I., Parametrized post-Newtonian theory of reference frames, multipolar expansions and equations of motion in the N-body problem. *Phys Rep*, 2004, 400:209–318
- 16 Will C. M., Nordtvedt, K. Jr., Conservation laws and preferred frames in relativistic gravity. I. preferred-frame theories and an extended PPN formalism. *Astrophys J*, 1972, 177, 757
- 17 Nordtvedt, K. Jr., Will C. M., Conservation laws and preferred frames in relativistic gravity. II. experimental evidence to rule out preferred-frame theories of gravity. *Astrophys J*, 1972, 177, 775
- 18 Blanchet L., Faye G., Ponsot B., Gravitational field and equations of motion of compact binaries to 5/2 post-Newtonian order. *Phys Rev D*, 1998, 58, 124002

- 19 Fischbach E., Talmadge C. L. The search for non-newtonian gravity. Springer-Verlag: New York Press, 1999
- 20 Will C. M. Theory and Experiment in Gravitational Physics. Cambridge: Cambridge University Press, 1993
- 21 Kidder L. E., Coalescing binary systems of compact objects to (post)^{5/2}-Newtonian order. V. Spin effects. *Phy Rev D*, 1995, 52, 821
- 22 Weisberg J. M., Taylor J. H., In Radio pulsars edited by Bailes M., Nice D. J., Thorsett S. Astronomical Society of the Pacific, San Francisco, 2003
- 23 Stairs I. H., Thorsett S. E., Taylor J. H., Wolszczan A., Studies of the relativistic binary pulsar PSR B1534+12. I. timing analysis. *Astrophys J*, 2002, 581:501–508
- 24 Kramer M., et al, Tests of general relativity from timing the double pulsar. *Science*, 314:97–102
- 25 Jacoby B. A., et al, Measurement of orbital decay in the double neutron star binary PSR B2127+11C. *Astrophys J Lett*, 2006, 644:L113–L116
- 26 Hulse R. A., Taylor J. H., Discovery of a pulsar in a binary system. *Astrophys J Lett*, 1975, 195:L51-L53
- 27 Adelberger E. G., Heckel B. R., Nelson A. E., Tests of the gravitational inverse-square law. *Ann. Rev. Nucl. Part. Sci.*, 2003, 53:77–121